UDC: 547.362:577.151.042
DOI: https://doi.org/10.30546/2521-6341.2026.01.908

SYNTHESIS OF ACETYLENIC ALCOHOLS BASED ON CYCLOPROPYLACETYLENE AND AROMATIC ALDEHYDES AND THEIR MOLECULAR DOCKING ANALYSIS AGAINST THE NOX2 RECEPTOR

Mirjalol E. ZIYADULLAEV[1]*, Suvonkul E. NURMANOV[2], Askar B. PARMANOV[2], Shavkatjon Sh. TURSUNOV[3], Odiljon E. ZIYADULLAEV

[1]*Chirchik State Pedagogical University, 111700, Uzbekistan*

[2]*National University of Uzbekistan named after Mirzo Ulugbek, 100174, Uzbekistan*

[3]*Jizzakh State Pedagogical University, 130100, Uzbekistan*

[4]*Tashkent Chemical-Technological Institute, 100011, Uzbekistan*

[5]*Alfraganus University, 100190, Uzbekistan*

Correspondence: e-mail:* ***ziyadullayev.91@mail.ru*

ARTICLE INFO

Article history:
Received:2025-11-23
Received in revised form: 2025-12-15
Accepted: 2026-01-18
Available online:2026-06-26

Keywords:
acetylenic alcohols, benzaldehyde, alkynylation reactions, catalytic system, enantioselective, Grignard reagent, reaction mechanism

ABSTRACT

In this research work, the nucleophilic addition reaction of cyclopropylacetylene with aromatic aldehydes was investigated in the presence of a catalytic system consisting of EtMgCl/$C_{17}H_{29}NO$/TFE. Within the scope of the study, the reactivity of benzaldehyde derivatives containing various functional groups (fluoro, chloro, bromo, alkyl, alkoxy, and hydroxyl) as well as structurally complex anthracene-9-carbaldehyde substrates was analyzed. The proposed synthetic method does not require expensive metals as catalysts or ultra-low temperatures. This methodology is considered cost-effective and convenient, enabling the preparation of structurally diverse acetylenic alcohols with high chemical yields (up to 91%). During the process, the primary factors influencing product yield and selectivity such as the composition of the catalytic system, stoichiometric ratios of the reagents, temperature, and reaction duration were systematically studied. It was demonstrated that 2,2,2-trifluoroethanol (TFE) serves to break down magnesium acetylide associates, thereby enhancing the reactivity of the in situ formed complex. A reaction mechanism for the alkynylation reaction, based on the cooperative effect of the ligand and the fluorine-containing components, was proposed. The electronic and steric effects of the substituents within the aldehydes were explained based on chemical principles. The structures and purity of the synthesized compounds were confirmed using ^{1}H, ^{13}C NMR spectroscopy.

1. INTRODUCTION

Aromatic acetylenic alcohols represent an important class of organic compounds containing an aromatic ring, an acetylenic (C≡C) bond, and a hydroxyl group within a single molecule. These compounds are widely utilized in the pharmaceutical industry, polymer chemistry, the synthesis of biologically active substances, and materials science [1-5].

In recent years, catalytic systems based on *ProPhenol* ligands and Me_2Zn have demonstrated high efficiency in the synthesis of aromatic acetylenic alcohols. The alkynylation reaction of heteroatom-containing aldehydes with phenylacetylene has been investigated using the *ProPhenol*/Me_2Zn catalytic system. As part of the research, the effects of reaction duration and temperature on product yield were systematically analyzed, and optimal reaction parameters were determined. Furthermore, the authors conducted a comparative study of the reactivity of various heteroatom-containing aldehydes, determining the influence of electronic and steric effects on reaction capability and product yield [6].

In the nucleophilic addition reaction of benzaldehyde and its halogenated derivatives with phenylacetylene, a complex catalytic system based on $Zn(OTf)_2$ and $TBAF{\cdot}3H_2O$ was employed. The influence of benzaldehyde and its halogen substituents on product yield was comprehensively analyzed. A reaction mechanism was proposed, and the reaction stages, activation energies, and kinetic characteristics were determined. Based on the selected catalytic system, relative efficiency series for the synthesis of aromatic acetylenic alcohols were proposed [7].

Lucke and his research group were the first to employ palladium complexes based on sydnones and sydnone imines in Sonogashira-Hagihara and Buchwald-Hartwig cross-coupling reactions. In this study, seven different Pd complexes were synthesized and their catalytic activities were investigated. The most effective results were achieved using the [*sydnon*-4-yl-$PdBr(PPh_3)_2$] complex, which provided a 100% yield in the reaction between phenyl bromide and 2-methylbut-3-yn-2-ol within 7 hours. It was highlighted that this result demonstrates shorter reaction times and higher efficiency when compared to the well-known $Pd(PhCN)_2Cl_2$/CuI/$P(t\text{-}Bu)_3$ catalytic system reported in the literature. In the study, ten different aromatic and heterocyclic acetylenic alcohols were synthesized, with thiophene, quinoline, phenanthrene, and anthracene derivatives obtained in high yields. The authors noted that although palladium complexes of sydnone imine derivatives required longer reaction times, they provided the best results for naphthalene derivatives [8].

New methods for the synthesis of vinyl ethers via modification of aromatic and aliphatic alkynes and acetylenic alcohols containing a triple bond have been developed [9], as well as new approaches for the synthesis of α-acrylamides based on nickel-catalyzed hydroalumination and nucleophilic addition reactions with isocyanates. This method allows for the efficient modification of both terminal and internal alkynes. The authors synthesized over 30 compounds with yields ranging from 70% to 98%. The reaction was conducted at 60°C for 2 hours, with substrate and reagent quantities optimized based on resource-efficiency principles. It was emphasized that this method requires lower temperatures and shorter reaction times compared to traditional Pd-catalyzed hydroamidation processes [10].

Ethynylation reactions of carbonyl compounds (aldehydes and ketones), imines, ketoesters, ketamine esters, oxycarbenes, and aldimines with various alkynes and their heteroatom derivatives have been studied in catalytic systems prepared on the basis of heavy metal (Zn, Au, Ag, Cu, Ti) salts and strong Lewis acids, and methods for the synthesis of new organic compounds have been developed [11-20].

2. RESULTS AND DISCUSSION

In this study, a series of *R*-substituted benzaldehyde derivatives containing alkyl, alkoxy, hydroxyl and halogen groups were selected. The alkynylation reactions were carried out with cyclopropylacetylene using the EtMgCl/$C_{17}H_{29}NO$/TFE catalytic system, resulting in the synthesis of the corresponding aromatic acetylenic alcohols (1-15). Reaction mechanisms for the synthesis of acetylene alcohols. The reaction was efficiently promoted by the EtMgCl/$C_{17}H_{29}NO$/TFE catalytic system at room temperature. The substrate scope utilized for this study included: Unsubstituted and alkyl-substituted benzaldehydes: Benzaldehyde and 4-ethylbenzaldehyde. Halogenated benzaldehydes - various isomers of fluoro- (2-F, 3-F, 4-F) and chloro-benzaldehydes (2-Cl, 3-Cl, 4-Cl), along with 3-(trifluoromethyl)benzaldehyde. Oxygenated and functionalized benzaldehydes - 4-butoxy-3-methylbenzaldehyde, 4-hydroxy-3-methylbenzaldehyde, 3,4,5-trimethoxybenzaldehyde, 2-bromo-4,5-dimethoxybenzaldehyde and 3,4-dihydroxy-5-methoxybenzaldehyde. Polycyclic aldehydes - anthracene-9-carbaldehyde.

Based on established literature sources [21-26], the reaction mechanism is proposed to involve the formation of a magnesium acetylide intermediate, which subsequently undergoes coordinated addition to the carbonyl group, stabilized by the synergistic effect of the chiral ligand and the trifluoroethanol (TFE) additive. The reaction scheme was proposed as follows:

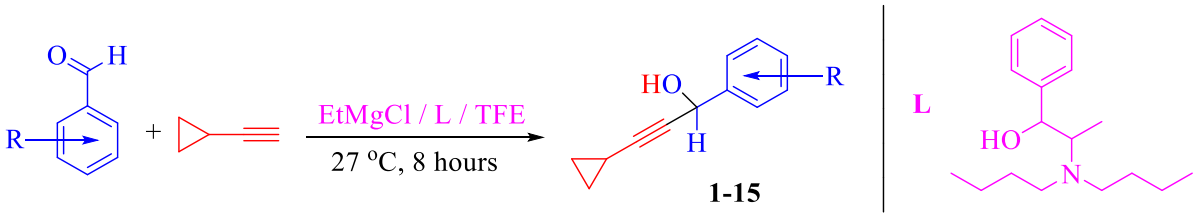

Fig. 1. *General reaction scheme for the synthesis of aromatic acetylenic alcohols*

Alkynylation reactions are proposed to occur through the following steps [27-29]. The catalytic process initiates with the in situ deprotonation of cyclopropyl acetylene to generate the active nucleophilic reagent. This preliminary stage involves the interaction of the terminal alkyne with EtMgCl in the presence of trifluoroethanol.

The ethyl group of the Grignard reagent acts as a strong base, deprotonating the acidic proton at the terminal position of the cyclopropyl acetylene. The subsequent evolution of ethane gas resulting from this acid-base interaction serves as the primary thermodynamic driving force, shifting the equilibrium toward the formation of the product. Consequently, a highly reactive intermediate, cyclopropylethynylmagnesium chloride, is successfully formed.

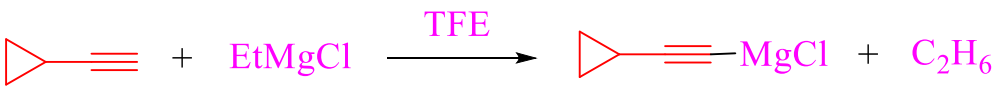

In the subsequent stage of the reaction, the coordination of the previously formed cyclopropylethynylmagnesium chloride intermediate with the chiral ligand is observed. The cyclopropylethynylmagnesium chloride establishes a coordination bond with the oxygen atom of the chiral ligand.

This complex chemical process leads to the formation of a cyclopropylethynylmagnesium alcoholate coordinated with both the chiral ligand and trifluoroethanol, accompanied by the elimination of hydrogen chloride from the system. This chiral complex serves as the primary

active catalytic species responsible for ensuring the enantioselective attack on the carbonyl group of the aldehyde in the following step.

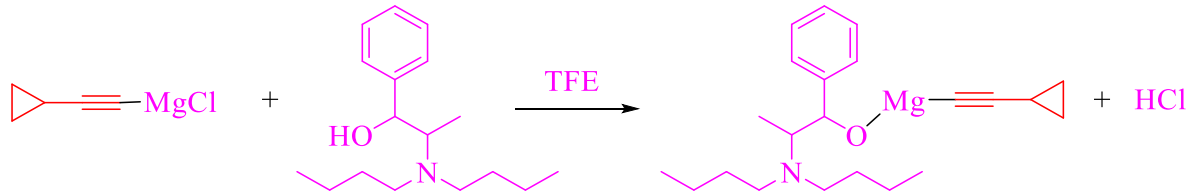

In the next step, the chiral magnesium alcoholate complex reacts with the aldehyde to form the new C-C bond. The carbonyl oxygen coordinates to the magnesium center, which triggers a significant increase in the electrophilicity of the carbonyl carbon. This activation makes the carbon atom highly susceptible to nucleophilic attack, effectively driving the reaction forward.

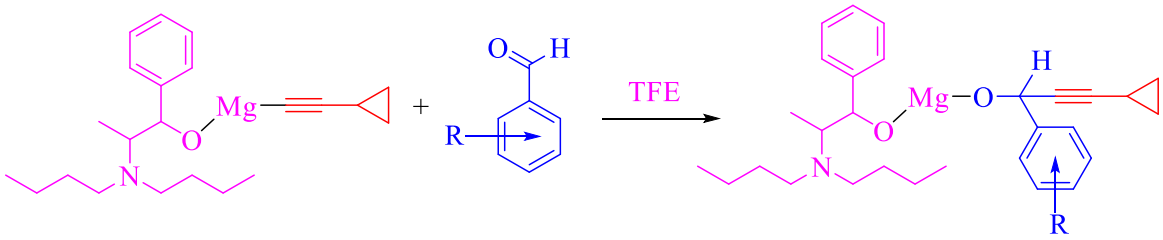

In the final stage, hydrolysis of the magnesium alcoholate intermediate leads to the cleavage of the magnesium oxygen (Mg-O) bond, followed by protonation. This process yields the target asymmetric propargyl alcohol and the magnesium hydroxide complex (L-Mg-OH). The liberation of the free alcohol effectively completes the catalytic cycle, allowing for the isolation of the chiral product in high optical purity.

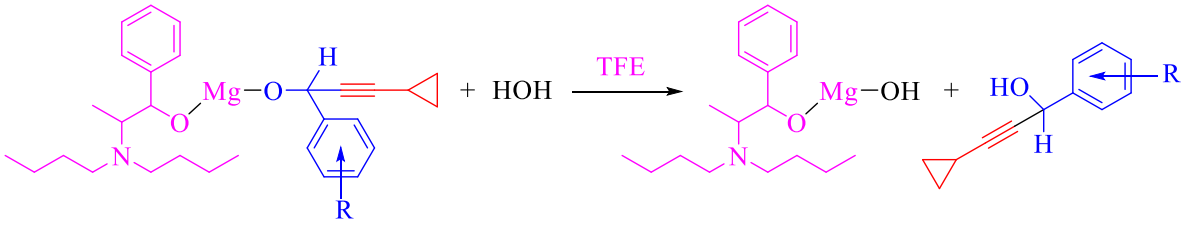

The reaction concludes with the formation of a magnesium hydroxide species (Mg-OH) and the recovery of the chiral ligand. This stage ensures the straightforward separation of the catalyst from the system and facilitates the final work-up procedure.

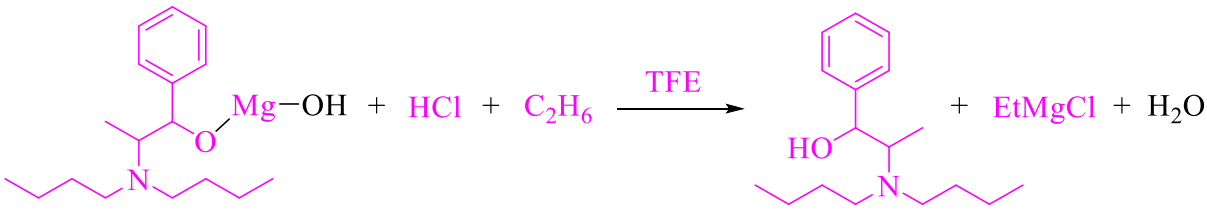

The overall process enables the regeneration of the catalyst and ensures the isolation of the final product with high optical purity. The alkynylation of aromatic aldehydes in the selected catalytic system was investigated within a temperature range of 10 to 40 °C for 4-12 hours. To qualitatively and quantitatively evaluate the influence of key parameters-such as temperature, reaction time, and reagent ratios on the process and product yield, a mathematical model was developed.

Optimization was conducted using the Box-Wilson method [30-31], which allowed for the determination of ideal conditions for achieving maximum yields. Based on experimental research results, it was established that the product is synthesized in high yields when the reaction is carried out for 8 hours at 25 ± 2 °C, using the selected substrate, reagent, catalyst, and ligand (aldehyde:alkyne:EtMgCl:L) in a molar ratio of 1:1.2:1.2:0.2 respectively.

Furthermore, the formation of intermediate and by-products was monitored to understand their impact on the reaction pathway. Some specific values of the synthesized acetylene alcohols were determined and the results obtained are presented in table 1.

Table 1. *Physicochemical characteristics of the synthesized aromatic acetylenic alcohols*

№	Gross formula	Molecular mass, g/mol	Product yield	System	R_f value
1	$C_{12}H_{12}O$	172	89.1	Hexane:EtOAc 10:1	14/37
2	$C_{14}H_{16}O$	200	84.3	Hexane:EtOAc 10:1	18/37
3	$C_{12}H_{11}OF$	190	88.2	Hexane:EtOAc 14:1	14/38
4	$C_{12}H_{11}OF$	190	91.0	Hexane:EtOAc 14:1	17/38
5	$C_{12}H_{11}OF$	190	85.3	Hexane:EtOAc 14:1	20/37
6	$C_{13}H_{11}OF_3$	240	86.5	Hexane:EtOAc 14:1	17/37
7	$C_{12}H_{11}OCl$	207	86.8	Hexane:EtOAc 14:1	14/37
8	$C_{12}H_{11}OCl$	207	89.3	Hexane:EtOAc 14:1	15/38
9	$C_{12}H_{11}OCl$	207	85.7	Hexane:EtOAc 14:1	12/38
10	$C_{17}H_{22}O$	258	88.1	Hexane:CH_2Cl_2 14:1	12/34
11	$C_{14}H_{16}O_2$	216	86.4	Hexane:CH_2Cl_2 14:1	17/37
12	$C_{15}H_{18}O_4$	262	88.3	Hexane:CH_2Cl_2 14:1	16/37
13	$C_{14}H_{15}O_3Br$	311	84.0	Hexane:CH_2Cl_2 14:1	15/37
14	$C_{13}H_{14}O_4$	234	82.3	Hexane:EtOAc 6:1	12/37
15	$C_{20}H_{16}O$	272	84.7	Hexane:EtOAc 6:1	15/37

Based on the data presented in the table, it can be noted that aromatic acetylenic alcohols containing various electron-donating and electron-acceptor substituents on the aromatic ring were synthesized from the corresponding aldehydes with yields ranging from 83% to 91%. It is particularly important to highlight that compounds 3, 4, and 5 have the same gross formula and are ortho-, meta-and para-isomers containing a fluorine atom as the substituent.

The difference in the yield among these isomers can be explained by considering mesomeric and inductive effects, along with the spatial hindrance created by the substituent. Thus, the nature and position of substituents on the aromatic aldehyde significantly affect the product yield. In

this case, when electron-acceptor groups (F, Cl) are in the para-position, the nucleophilic attack of the alkyne on the carbonyl group is facilitated due to the increased electrophilicity of the carbonyl carbon atom, thereby ensuring the synthesis of the target acetylenic alcohols in high yields (90-91%).

Conversely, substituents in the ortho-position create steric hindrance, which leads to a decrease in product yield (83-85%). The structural identities of the resulting aromatic acetylenic alcohols were confirmed by spectroscopic methods.

The quantum chemical properties of the synthesized aromatic acetylenic alcohols were calculated using modern software.

Table 2. *Results of quantum chemical calculations of synthesized aromatic acetylenic alcohols*

Aromatic acetylene alcohols	Thermal energy, kcal/mol	Van der Waals energy, kcal/mol	Clone energy, kcal/mol	Torsion energy, kcal/mol	Valence angle energy, kcal/mol	Bond energy, kcal/mol
1	4.5147	6.0312	0.2554	-3.1905	0.388	1.2859
2	5.0340	4.6142	0.9875	-3.9569	0.5293	2.8599
3	0.0921	2.3387	-0.8067	-3.2518	0.2786	1.5332
4	3.2833	2.9637	1.3050	-3.1351	0.2874	1.8622
5	3.2491	2.9955	1.2681	-3.1279	0.2822	1.8313
6	8.8165	3.9246	1.3850	0.7888	0.416	2.3022
7	-0.4868	0.1116	-0.0390	-2.9379	0.4655	1.9132
8	2.4977	2.9276	0.9284	-3.2152	0.2862	1.5708
9	2.6468	3.0885	0.8892	-3.2089	0.2881	1.5899
10	11.9322	7.7509	1.1262	-2.6518	0.9692	4.7378
11	8.4417	5.5218	0.5748	-1.0785	0.6706	2.7530
12	21.6591	9.6203	0.7419	4.1066	1.5103	5.6800
13	13.4099	7.1512	-0.3697	0.1108	1.0848	5.4339
14	-3.7365	-2.1157	-2.1653	-6.0052	6.661	5.8887
15	1.2286	15.602	0.8156	-21.1261	1.7476	4.1893

Table 2 presents the calculated molecular mechanics and energy parameters for compounds 1-15. These parameters were investigated to evaluate the conformational stability and potential spatial interactions of the synthesized aromatic acetylenic alcohols. The obtained values represent the intramolecular strain occurring during structural rearrangements. In particular, compound 15 possesses a high negative torsion energy and a significant Van der Waals contribution due to its stable anthracene core. These quantum chemical values correlate well with the geometric complementarity and binding strength observed in the molecular docking studies against the active site of the receptor.

Molecular docking. The molecular docking method is an essential tool in contemporary pharmaceutical research for examining the interactions between biologically active substances and their target proteins. This method makes it possible to assess a ligands thermodynamic stability and capacity for binding to the protein. The stability of the ligand-protein complex is reflected in the binding free energy ($\Delta G_{binding}$) determined by docking software; the stronger the binding interaction, the more negative the value [32].

This work investigated how the synthesized aromatic acetylenic alcohol derivatives interacted with the core human NADPH oxidase NOX2 enzyme (PDB ID: 7U8G) using the AutoDock Vina algorithm. The NOX2 enzyme serves as a critical biological target associated with oxidative stress and cellular signaling pathways. Using molecular docking, the binding energies of the synthetic compounds with the target NOX2 receptor were determined. Negative ΔG values indicate the thermodynamic stability of the ligand-protein complex formation, the energy values are stated in kilocalories per mole (kcal/mol). For every compound (1-15), table 3 methodically compiles the calculated relative binding energy values.

Table 3. Binding energies of the synthesized aromatic acetylenic alcohols with the 7U8G structure of the core human NADPH oxidase NOX2

№ (AAA)	Docking Score (kcal/mol)	№ (AAA)	Docking Score (kcal/mol)	№ (AAA)	Docking Score (kcal/mol)
1	-7.1	6	-8.1	11	-7.2
2	-7.1	7	-7.2	12	-6.9
3	-7.2	8	-7.2	13	-6.7
4	-7.2	9	-7.1	14	-6.8
5	-7.1	10	-7.3	15	-8.2

With a value of -8.2 kcal/mol, compound 15 displayed the lowest binding energy among the synthesized compounds with the 7U8G (NOX2) receptor. This outcome suggests that with NOX2, this molecule can create the most energetically favorable and stable complex. Among the high-affinity ligands are also compound 6 (-8.1 kcal/mol) and compound 10 (-7.3 kcal/mol). Their binding energies demonstrate strong affinity and excellent structural complementarity within the target active cavity. By contrast, compound 13 displayed the lowest binding with the 7U8G receptor at -6.7 kcal/mol. This value indicates fewer interactions between the ligand and the receptor since it is much higher than those of the other compounds.

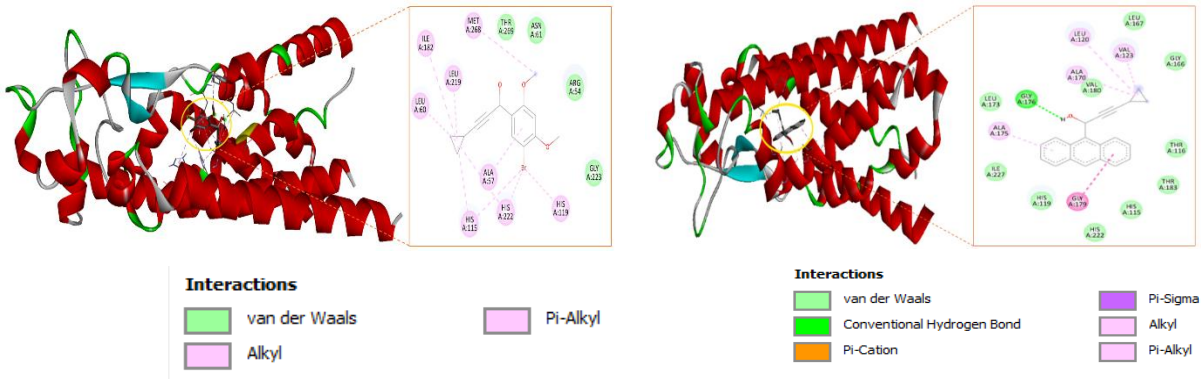

***Fig.* 2.** *Comparison of molecular docking poses and 2D interaction diagrams of the highest-scoring compound (15) and the lowest-scoring compound (13) within the active site of the core human NADPH oxidase NOX2 (PDB ID: 7U8G)*

The obtained results and the analysis of the ligand-protein complex presented in figure 2 indicate that among all synthesized derivatives, 1-(anthracen-9-yl)-3-cyclopropylprop-2-yn-1-ol (15) exhibited the highest binding affinity (8.2 kcal/mol). According to the 2D interaction diagram, the hydroxyl group of compound 15 forms a stable hydrogen bond with the Met268 amino acid residue. Meanwhile, the anthracene fragment forms a specific π-cation bond with the Arg54 residue and a π-sigma interaction with the Ala57 residue. Additionally, the cyclopropyl ring of the molecule engages in a π-alkyl interaction with the Tyr29 residue, ensuring the stability of the complex. Conversely, in compound 13, which exhibited the lowest binding energy, the

interactions within the active site of the protein are mainly restricted to spatial constraints and alkyl contacts of the cyclopropyl ring, the aromatic core, and the bromine atom of the molecule with Leu60, Leu219, Ala57, His115, His222, and His119 residues, indicating that the ligand could not achieve an energetically favorable orientation within the active site of the protein. The high binding affinity of compound 15 correlates well with its geometric and electronic properties. According to the quantum chemical calculations, this compound demonstrated the highest Van der Waals energy (15.60 kcal/mol) and a significant negative torsion energy (-21.12 kcal/mol). These parameters ensure the conformational stability of the ligand and its effective spatial interaction with specific hydrophobic regions of the protein. The complex and bulky structure of the anthracene fragment not only promotes a stable complex formation within the active site of the protein but also facilitates the transition of the molecule into an energetically favorable conformation. Furthermore, the synthesis of compound 15 with a high yield demonstrates a correlation between its chemical reactivity and biological activity potential.

3. EXPERIMENTAL PARTS

IR spectra were recorded on a Perkin-Elmer Spectrum 2000 FT-IR spectrometer using KBr pellets. ^{1}H NMR (400 MHz) spectra were recorded on a Bruker AMX spectrometer using $CDCl_3$ or C_6D_{12} as solvents, with TMS or GMDS as internal standards (δ-scale). Solvents were evaporated using Heidolph Hei-VAP Core and Expert rotary evaporators. Crude products were purified by flash or column chromatography on silica gel 60, employing various organic solvents as eluents. The progress of the reactions and product purity were monitored by thin-layer chromatography (TLC).

Synthesis of 3-cyclopropyl-1-phenylpropyn-2-ol-1 using the EtMgCl/$C_{17}H_{29}NO$/TFE catalytic system (1): A 50 mL dry vial equipped with a magnetic stir bar was charged with 10 mL of 2,2,2-trifluoroethanol (TFE). To this solution, ethylmagnesium chloride (1.07 g, 12 mmol) and cyclopropylacetylene (0.79 g, 12 mmol) were added sequentially. The mixture was stirred for 60 min at room temperature to facilitate the formation of the magnesium acetylide intermediate. Subsequently, the chiral ligand 2-(dibutylamino)-1-phenylpropan-1-ol (0.53 g, 2 mmol) and benzaldehyde (1.06 g, 10 mmol) were added, followed by a catalytic amount of hydroquinone to prevent polymerization. The reaction mixture was stirred for 8 hours at ambient temperature. Upon completion, the mixture was quenched with water and stirred for an additional 3 hours to ensure complete hydrolysis. The crude product was extracted with dichloromethane (3×10 mL), and the combined organic layers were dried over anhydrous Na_2SO_4. The solvents were removed under reduced pressure by simple distillation. The resulting residue was further purified by column chromatography on silica gel using a mixture of n-hexane and ethyl acetate (10:1) as the eluent to afford the pure product 3-cyclopropyl-1-phenylprop-2-yn-1-ol (1) in 89.1 % (1.53 g) yield.

The remaining aromatic acetylenic alcohols were synthesized according to this general procedure. The ^{1}H NMR spectra confirming the structures of the synthesized compounds and their structural formulas are presented below.

3-cyclopropyl-1-phenylprop-2-yn-1-ol (**1**). ^{1}H NMR (400 MHz, $CDCl_3$) δ 7.48-7.23 (m, 5H, Ar-H), 5.78-5.52 (m, 2H, CH-OH and OH), 2.68 (td, *J*=7.0, 2.5 Hz, 1H, CH-cyclopropyl), 1.55-1.33 (m, 4H, cyclopropyl).

3-cyclopropyl-1-(4-ethylphenyl)prop-2-yn-1-ol (**2**). ^{1}H NMR (400 MHz, $CDCl_3$) δ 7.35-7.26 (m, 2H), 7.19 (dt, J=7.5, 1.0 Hz, 2H), 5.73-5.44 (m, 2H), 2.75-2.55 (m, 3H), 1.45 (dd, *J*=7.1, 2.4 Hz, 4H), 1.23 (t, *J*=8.0 Hz, 3H).

3-cyclopropyl-1-(2-fluorophenyl)prop-2-yn-1-ol (**3**). ^{1}H NMR (400 MHz, $CDCl_3$) δ 7.53-7.27 (m, 2H), 7.27-7.16 (m, 2H), 5.84 (dd, *J*=6.7, 2.5 Hz, 1H), 5.64 (d, *J*=6.8 Hz, 1H), 2.65 (pd, *J*=7.1, 2.6 Hz, 1H), 1.53-1.34 (m, 4H).

3-cyclopropyl-1-(3-fluorophenyl)prop-2-yn-1-ol (**4**). ^{1}H NMR (400 MHz, $CDCl_3$) δ 7.39 (td, *J*=7.5, 5.0 Hz, 1H), 7.23 (ddt, *J*=22.4, 7.9, 1.5 Hz, 2H), 7.01 (tt, *J*=7.8, 1.6 Hz, 1H), 5.72 (d, *J*=6.7 Hz, 1H), 5.61 (dd, *J*=6.7, 2.5 Hz, 1H), 2.67 (pd, *J*=7.1, 2.6 Hz, 1H), 1.53-1.28 (m, 4H).

3-cyclopropyl-1-(4-fluorophenyl)prop-2-yn-1-ol (**5**). ^{1}H NMR (400 MHz, $CDCl_3$) δ 7.68-7.56 (m, 2H), 7.33-7.22 (m, 2H), 5.84 (d, *J*=6.7 Hz, 1H), 5.78 (dd, *J*=6.7, 2.5 Hz, 1H), 2.84 (pd, *J*=7.1, 2.5 Hz, 1H), 1.69-1.46 (m, 4H).

3-cyclopropyl-1-(3-(trifluoromethyl)phenyl)prop-2-yn-1-ol (**6**). ^{1}H NMR (400 MHz, $CDCl_3$) δ 7.59 (t, *J*=1.4 Hz, 1H), 7.49 (dt, *J*=7.5, 1.6 Hz, 1H), 7.30 (t, *J*=7.5 Hz, 1H), 7.21 (dt, *J*=7.5, 1.5 Hz, 1H), 5.62 (d, *J*=6.6 Hz, 1H), 5.50 (dd, *J*=6.7, 2.5 Hz, 1H), 2.47 (pd, *J*=7.0, 2.5 Hz, 1H), 1.51-1.18 (m, 4H).

1-(2-chlorophenyl)-3-cyclopropylprop-2-yn-1-ol (**7**). ^{1}H NMR (400 MHz, $CDCl_3$) δ 7.61-7.38 (m, 2H), 7.34-7.18 (m, 2H), 5.83 (dd, J=7.0, 2.5 Hz, 1H), 5.49 (d, *J*=7.0 Hz, 1H), 2.62 (m, *J*=7.0, 2.6 Hz, 1H), 1.49-1.21 (m, 4H).

1-(3-chlorophenyl)-3-cyclopropylprop-2-yn-1-ol (**8**). ^{1}H NMR (400 MHz, $CDCl_3$) δ 7.50-7.32 (m, 2H), 7.26 (tt, *J*=7.1, 1.5 Hz, 2H), 5.95-5.12 (m, 2H), 2.61 (pd, *J*=7.0, 2.2 Hz, 1H), 1.60-0.96 (m, 4H).

1-(4-chlorophenyl)-3-cyclopropylprop-2-yn-1-ol (**9**). ^{1}H NMR (400 MHz, $CDCl_3$) δ 7.53-6.97 (m, 4H), 5.66-5.19 (m, 2H), 2.57 (pd, *J*=7.1, 2.5 Hz, 1H), 1.37-1.28 (m, 4H).

1-(4-butoxy-3-methylphenyl)-3-cyclopropylprop-2-yn-1-ol (**10**). ^{1}H NMR (400 MHz, $CDCl_3$) δ 7.36-7.14 (m, 2H), 6.84 (d, *J*=7.4 Hz, 1H), 5.74 (d, *J*=6.6 Hz, 1H), 5.63 (dd, *J*=6.7, 2.5 Hz, 1H), 4.02 (t, *J*=7.0 Hz, 2H), 2.58 (pd, *J*=7.0, 2.4 Hz, 1H), 2.17 (s, 3H), 1.79-1.65 (m, 2H), 1.60-1.20 (m, 6H), 0.99 (t, *J*=8.0 Hz, 3H).

3-cyclopropyl-1-(4-methoxy-3-methylphenyl)prop-2-yn-1-ol (**11**). ^{1}H NMR (400 MHz, $CDCl_3$) δ 7.56-7.19 (m, 2H), 6.80 (d, *J*=7.5 Hz, 1H), 5.71 (d, *J*=6.8 Hz, 1H), 5.57 (dd, *J*=6.7, 2.5 Hz, 1H), 3.87 (s, 3H), 2.61 (pd, *J*=7.0, 2.6 Hz, 1H), 2.19 (s, 3H), 1.57-1.35 (m, 4H).

3-cyclopropyl-1-(3,4,5-trimethoxyphenyl)prop-2-yn-1-ol (**12**). ^{1}H NMR (400 MHz, $CDCl_3$) δ 7.35-7.18 (m, 2H), 5.34 (s, 9H), 4.11 (pd, *J*=7.1, 2.5 Hz, 1H), 3.00-2.78 (m, 4H).

1-(5-bromo-2,4-dimethoxyphenyl)-3-cyclopropylprop-2-yn-1-ol (**13**). ^{1}H NMR (400 MHz, $CDCl_3$) δ 7.64 (s, 1H), 6.64 (s, 1H), 5.83 (dd, *J*=7.0, 2.6 Hz, 1H), 5.48 (d, *J*=7.0 Hz, 1H), 3.87 (d, *J*=34.1 Hz, 6H), 2.59 (m, *J*=7.0, 2.6 Hz, 1H), 1.66-0.87 (m, 4H).

4-(3-cyclopropyl-1-hydroxyprop-2-yn-1-yl)-5-methoxybenzene-1,2-diol (**14**). ^{1}H NMR (400 MHz, $CDCl_3$) δ 8.65 (s, 1H), 8.54 (s, 1H), 6.96 (s, 1H), 6.50 (s, 1H), 5.74 (dd, *J*=7.0, 2.5 Hz, 1H), 5.48 (d, *J*=7.0 Hz, 1H), 3.83 (s, 3H), 2.59 (pd, *J*=7.0, 2.6 Hz, 1H), 1.52-1.24 (m, 4H).

(R)-1-(anthracen-9-yl)-3-cyclopropylprop-2-yn-1-ol (**15**). ^{1}H NMR (400 MHz, $CDCl_3$) δ 8.27 (dd, *J*=7.3, 1.6 Hz, 2H), 8.15 (tt, *J*=1.5, 0.7 Hz, 1H), 7.81 (dt, *J*=7.5, 1.7 Hz, 2H), 7.30 (m, *J*=25.4, 7.5, 1.6 Hz, 4H), 5.95 (dd,*J*=6.9,2.5 Hz, 1H), 5.47(d, *J*=6.8 Hz, 1H), 2.39(pd, *J*=7.0, 2.5 Hz, 1H), 1.34-0.98 (m, 4H).

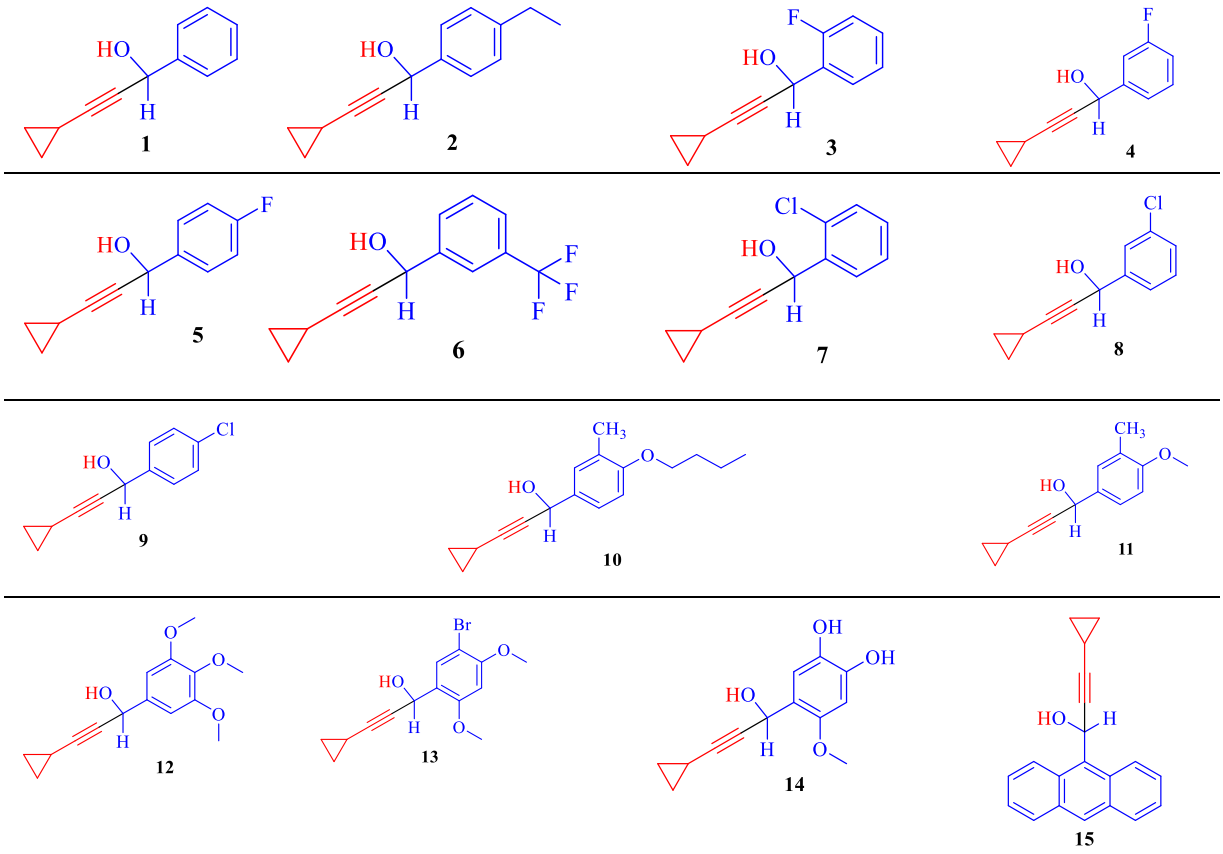

Fig. 3. *Structural formula of synthesized aromatic acetylenic alcohols*

3.1. Molecular docking

Molecular docking simulations were performed using the AutoDock Vina algorithm. The cryo-EM structure of the human NOX2 enzyme (PDB ID: 7U8G) was obtained from the PDB. The grid box was centered at x=143.337, y=143.645, z=141.271 with dimensions of 40×40×40 Å. The exhaustiveness parameter was set to 64. Visualization of the docking poses was conducted using BIOVIA Discovery Studio 2020 and PyMOL.

4. CONCLUSION AND RECOMMENDATIONS

For the first time, a series of new aromatic acetylenic alcohols were synthesized via the enantioselective alkynylation of benzaldehyde and its various derivatives using cyclopropylacetylene in the presence of an EtMgCl/$C_{17}H_{29}NO$/TFE catalytic system. The influence of the spatial structure of aldehyde molecules, the nature of their substituents, and their stability on the product yield and reaction rate were thoroughly investigated. The synthesized compounds were identified and characterized using modern physicochemical methods; their purity and structural properties were confirmed, and reaction mechanisms were proposed based on energetic and quantum-chemical calculations. These acetylenic alcohols, possessing both a hydroxyl group and a highly reactive triple bond, hold significant practical potential in fine organic synthesis, polymer chemistry, and the development of biologically active agents for pharmaceutical and agricultural applications against various bacteria and fungi.

REFERENCES

1. Jiang, M., Guo, H., Wu, Q., Lu, X., Zou, Y., Fu, Q., Chen, S., Liu, L., & Peng, B. (2023). Anti-inflammatory acetylenic meroterpenoids from the ascidian-derived fungus Amphichorda felina SYSU-MS7908. *Bioorganic Chemistry*, 139, 106715.
2. Sfameni, S., Rando, G., Rosaria, M., & Plutino, M. R. (2023). Sustainable Secondary-Raw Materials, Natural Substances and Eco-Friendly Nanomaterial-Based Approaches for Improved Surface Performances: An Overview of What They Are and How They Work. *International Journal of Molecular Sciences*, 24, 5472.
3. Ghobakhloo, S., Khoshakhlagh, A. H., Morais, S., & Tehrani, A. M. (2023). Exposure to Volatile Organic Compounds in Paint Production Plants: Levels and Potential Human Health Risks. *Toxics*, 11, 111.
4. Lo, Y. H., Umeda, K., Kurisawa, N., Jeelani, G., Nozaki, T., & Suenaga, K. (2023). Total synthesis of acetylene-containing lipopeptides odookeanynes A and B. *Tetrahedron Letters*, 130, 154763.
5. Ji, A., Shafique, B., Xu, J., Xie, J., & Ding, Z. (2025). Recent Developments in Synthesis, Functionality, and Sustainability of Metal-Organic Framework Films for Fruits and Vegetables Packaging. *Trends in Food Science & Technology*, 166, 105392.
6. Otamukhamedova, G. K., Ziyadullaev, O. E., Salieva, M. K., Boltayeva, R. A., Faizullaev, R. K., Sayfieva, Y. U., Mukhlisa, N. E., & Omonova, D. (2025). Synthesis and Characterization of Acetylene Alcohols Via Alkynylation of Heteroatomic Aldehydes with Phenylacetylene Under Various Reaction Parameters Completed with Spatial Chemical Structure, Literature Review, and Bibliometric Analysis. *ASEAN Journal of Science and Engineering*, 5, 61-76.
7. Otamukhamedova, G. K., Ziyadullaev, O. E., Buriev, F. K., Ablakulov, L. Q., & Khaitov, J. K. (2026). Enantioselective alkylnylation of cyclopentanone: Synthesis, dimerization, and cross-coupling transformations of 1-ethynylcyclopentan-1-ol. *Chemical Review and Letters*, 9(2), 192-200.
8. Lucke, A.-L., Pruschinski, L., Freese, T., & Schmidt, A. (2020). Sonogashira-Hagihara and Buchwald-Hartwig cross-coupling reactions with sydnone and sydnone imine derived catalysts. *Arkivoc*, 2020(vii), 94-104.
9. Ziyadullaev, M. E., Tursunov, S. S., Parmanov, A. B., Nurmanov, S. E., Abdullaev, J. U., Abduraxmanova, S. S., Toshov, K. S., Abduxaliqov, F. J., Khudiyarova, G. S., & Musaev, K. B. (2026). Efficient synthesis of N-phenylbenzamides via amidation of vinyl esters of aromatic carboxylic acids with aniline. *Chemical Problems*, 24(4), 591-598.
10. Park, C. H., Lim, S., Jung, B., & Lee, Y. (2025). Regioselective Formal Hydroamidation of Alkynes: Synthesis of α-Substituted Acrylamides. *European Journal of Organic Chemistry*, e202401234.
11. Mammadov, E. I., & Zaidova, G. A. (2025). New synthesis of butane and cyclohexane compounds containing two furan fragments. *Azerbaijan Technical University Journal*, 9(1), 471-478.
12. Li, J., Yao, Z., Zhao, J., Deng, S., Wang, S., & Wang, J. (2023). Microkinetic simulations of acetylene(acetylene-d2) hydrogenation (deuteration) on Ag nanoparticles. *Molecular Catalysis*, 535, 112845.
13. Lionus Leo, G. M., Murugapoopathi, S., Thodda, G., Baligidad, S. M., Jayabal, R., Nedunchezhiyan, M., & Devarajan, Y. (2023). Optimisation and environmental analysis of waste cashew nut shell oil biodiesel/cerium oxide nanoparticles blends and acetylene fumigation in agricultural diesel engine. *Sustainable Energy Technologies and Assessments*, 58, 103375.
14. Balyan, S., Jiang, C., Caiola, A., & Hu, J. (2023). Microwave catalytic conversion of acetylene for co-production of hydrogen and carbon nanotubes. *Chemical Engineering Journal*, 454, 140115.
15. Alonso, D. A., Macia, B., Pastor, I. M., & Baeza, A. (2024). Recent Advances on the Catalytic Asymmetric Allylic α-Alkylation of Carbonyl Derivatives Using Free Allylic Alcohols. *ACS Organic & Inorganic Au*, 4(3), 269-286.
16. Shaw, R., Singh, A., Althagafi, I., Pratap, R., & Yadav, D. K. (2025). The stereo-divergent functionalization of alkynes: a comprehensive review. *RSC Advances*, 15, 12202-12245.
17. Trost, B. M., & Weiss, A. H. (2009). The Enantioselective Addition of Alkyne Nucleophiles to Carbonyl Groups. *Advanced Synthesis & Catalysis*, 351, 963-983.
18. Li, H., Zhang, E., Fan, J., Yuan, N., Liu, T., & Liu, C. (2025). Synthesis of conjugated enyne sulfones by three-component coupling of acetylenic sulfones, diethylzinc and terminal alkynes under metal-free catalyst. *Journal of Organic Chemistry*, 1038, 123746.

19. Gein, V. L., Nosova, N. V., Yankin, A. N., Bazhina, A. Y., & Dmitriev, M. V. (2019). Stereoselective synthesis of novel functionalized cyclohexanone derivatives via the condensation of aromatic aldehydes with acetoacetamide and the influence of the ortho-effect and autocondensation. *Tetrahedron Letters*, 60, 1592-1596.
20. Mu, Y., Yan, L., Chu, B., Zhong, S., Fan, J., & Cheng, Y. (2023). Prediction of solubility of acetylene in organic solvents over a wide range of temperature and pressure. *Chemical Engineering Science*, 276, 118824.
21. Park, C. H., Lim, S., Jung, B., & Lee, Y. (2025). Regioselective Formal Hydroamidation of Alkynes: Synthesis of α-Substituted Acrylamides. *European Journal of Organic Chemistry*, 28, e202401484.
22. Ohshima, T., Kawabata, T., Takeuchi, Y., Kakinuma, T., Iwasaki, T., & Yonezawa, T. (2019). C1-Symmetric Rh/Phebox-Catalyzed Asymmetric Alkynylation of α-Ketoesters. *Angewandte Chemie International Edition*, 50, 6296-6300.
23. Lo, V. K., Liu, Y., Wong, M. K., & Che, C. M. (2016). Gold (III) Salen Complex-Catalyzed Synthesis of Propargylamines via a Three-Component Coupling Reaction. *Organic Letters*, 8, 1529-1532.
24. Mi, Z., Tang, J., Guan, Z., Shi, W., & Chen, H. (2018). Cleavage of C–C and C–O Bonds to Form C–C Bonds: Direct Cross-Coupling between Acetylenic Alcohols and Benzylic. *European Journal of Organic Chemistry*, 2018, 4479-4482.
25. Juhász, K., Magyar, Á., & Hell, Z. (2020). Transition-Metal-Catalyzed Cross-Coupling Reactions of Grignard Reagents. *Synthesis*, 52, A-T.
26. Shikhaliyev, N. Q., Qajar, A. M., Ahmedova, N. E., Garazade, K. A., Maharramov, A. M., Shikhaliyeva, I. M., & Niyazova, A. A. (2024). Methanolysis of dichlorodiazadienes synthesized based on 4-methylbenzaldehyde. *Journal of Baku Engineering University-Advances in Chemistry and Chemical Engineering*, 8(1), 67-76.
27. Takahashi, R., Hu, A., Gao, P., Gao, Y., Pang, Y., Seo, T., Jiang, J., Maeda, S., Takaya, H., Kubota, K., & Ito, H. (2021). Mechanochemical Synthesis of Magnesium-Based Carbon Nucleophiles in air and their use in Organic Synthesis. *Nature Communications*, 12, 6691-6701.
28. Lu, Z., & Ma, S. (2006). Studies on the Cu(I)-Catalyzed Regioselective anti-Carbometallation of Secondary Terminal Propargylic Alcohols. *Journal of Organic Chemistry*, 71, 2655-2660.
29. Jiang, Y., Ma, Y., Ma, E., & Li, Z. (2019). Copper-Catalyzed Selective Cross-Couplings of Propargylic Ethers with Aryl Grignard Reagents. *Asian Journal of Organic Chemistry*, 8, 1834-1837.
30. Ziyadullaev, M. E., Karimov, R. K., Zuhurova, G. V., Abdurazakov, A. S., & Sagdullaev, S. S. (2020). Optimizatsiya protsessa sinteza 6-nitro-3,4-dihidrokhinazolin-4-ona. *Izvestiya vysshikh uchebnykh zavedeniy. ChemChemTech*, 63(7), 48-53.
31. Kumar, R. (2022). Response surface methodology (RSM): An overview to analyze multivariate data. *Indian Journal of Microbiology Research*, 9(4), 241-248.
32. Liu, R., Song, K., Wu, J.-X., Geng, X.-P., Zheng, L., Gao, X., Peng, H., & Chen, L. (2022). Structure of human phagocyte NADPH oxidase in the resting state. *eLife*, 11, e83743.